Pergamon

Int. J. Solids Structures Vol. 31, No. 20, pp. 2867–2881, 1994

0020–7683/94 $7.00 + .00

0020–7683(93)E0007–5

AN IMPROVED IN-PLANE THERMOELASTIC THEORY FOR LAMINATED COMPOSITE PLATES

LIU PING, ZHANG YONGWEI and ZHANG XIANGZHOU
Aircraft Department, Northwestern Polytechnical University, Xi'an 710072, People's Republic of China

(*Received* 19 *June* 1992; *in revised form* 21 *October* 1993)

Abstract—A new laminated plate thermoelastic theory based upon a new mixed variational principle proposed by Reissner [*Int. J. Numer. Meth. Engng* **20,** 1366–1368 (1984)] is developed to study the thermal stresses of laminated composite plates. Across each individual layer, piecewise linear continuous displacement and quadratic transverse shear stress distributions are assumed. The temperature variation through the thickness is considered to be linear. The theory is examined by applying it to the problem of rectangular plate bending. Some numerical results for thermal stresses and deflections are compared with those obtained using the high-order and the first-order zig-zag thermoelastic theories.

NOMENCLATURE

$(\ )^{(k)}$	$= 1, 2, \ldots, N$	quantities associated with the kth layer
$n^{(k)}h$		thickness of the kth layer
$(\ )_{,i}$		partial differentiation with respect to x_i
$u_i^{(k)}$		displacement vector
$\sigma_{ij}^{(k)}$		stress tensor
$e_{ij}^{(k)}$		strain tensor
$f_i^{(k)}$		body force
$\alpha_i^{(k)}$		linear thermal expansion coefficient of the kth layer in principal axis directions
ΔT		temperature change
$A^{(k)}$		the x_3 domain occupied by the kth layer
$\bar{C}_{ij}^{(k)}$		reduced stiffness of the kth layer

1. INTRODUCTION

Tremendous interest in the analysis of thermoelastic behavior of laminated composite plates has emerged in recent years. This interest is due to the increased use of high-modulus, high-strength and low-weight composite materials in aerospace and various fields of modern technology.

The problem of thermal bending of anisotropic plates was first studied by Pell (1946), who derived the equations governing the transverse deflection of a thin plate. Stavsky (1963) used a general thermoelastic theory for thin heterogeneous anisotropic plates to obtain deformations and stresses in a thin rectangular plate simply supported along two infinitely long edges and subject to uniform heating (also see Stavsky, 1975). Whitney and Ashton (1971) studied the effects of moisture on the elastic response of layered composite plates. The moisture effects enter the mathematical formulation in the same form as the thermal effect. Thermally induced deformations and stress resultants in symmetric laminated plates were analysed by Wu and Tauchert (1980a, b). The method of Levy is used to study the transverse bending of specially orthotropic laminates having two opposite edges simply supported and subject to a temperature distribution using the classical laminate theory. In Wu and Tauchert (1980a, b), thermal deformations and stress resultants in rectangular, antisymmetric cross-ply and angle-ply laminates were investigated. For more general arrangements of the laminae, approximate methods of stress analysis, such as the Rayleigh–Ritz technique, were used in Wu (1978). A finite element formulation of the equations of the first-order theory of anisotropic composite plates subjected to thermal and mechanical loadings was presented by Reddy and Hsu (1980).

Most of the theories discussed so far, which are classified as displacement-based theories, suffer from a common deficiency: constitutive equations lead to discontinuous interlaminar stresses. This shortcoming can be overcome by the improved in-plane thermoelastic response theory, which is based upon Reissner's (1984) mixed variational principle, by taking the transverse stresses to be quadratic functions of a local thickness coordinate and assuming piecewise continuous in-plane displacement distributions across each layer. The advantage of using Reissner's mixed variational principle is that it automatically yields the appropriate shear correction factors for the transverse shear constitutive equations.

This report investigates the thermal stresses and deflections of laminated plates using the improved in-plane thermoelastic theory and compares the results with those obtained using the high-order and the first-order zig-zag theories.

2. IMPROVED IN-PLANE THERMOELASTIC THEORY

Formulation

Consider an N-layer laminated composite plate of uniform thickness h, as shown in Fig. 1. A Cartesian coordinate system is chosen such that the middle surface of the plate occupies a domain D in the x_1, x_2 plane, the x_3 axis being normal to this plane. Volume fractions $n^{(k)}$ satisfy the relation:

$$\sum_{k=1}^{N} n^{(k)} = 1. \tag{1}$$

Unless otherwise specified, the usual Cartesian indicial notation is employed where Latin and Greek indices range from 1 to 3 and 1 to 2, respectively. Repeated indices imply the summation convention.

The governing equations associated with the kth layer are:

(a) Equilibrium equations

$$\sigma_{ji,j}^{(k)} + f_i^{(k)} = 0; \quad \sigma_{ji}^{(k)} = \sigma_{ij}^{(k)}. \tag{2}$$

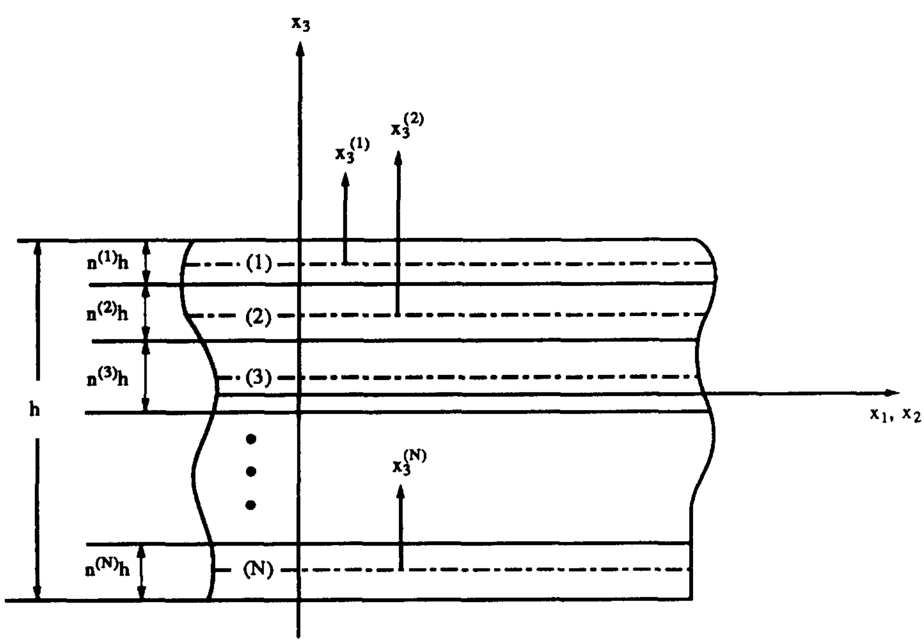

Fig. 1. Plate geometry and coordinate system.

(b) Constitutive equations

(I) principal axis constitutive equations for orthotropic layers

$$\begin{bmatrix}\sigma_1\\ \sigma_2\\ \sigma_3\\ \sigma_4\\ \sigma_5\\ \sigma_6\end{bmatrix}^{(k)} = \begin{bmatrix}Q_{11} & Q_{12} & Q_{13} & 0 & 0 & 0\\ Q_{12} & Q_{22} & Q_{23} & 0 & 0 & 0\\ Q_{13} & Q_{23} & Q_{33} & 0 & 0 & 0\\ 0 & 0 & 0 & Q_{44} & 0 & 0\\ 0 & 0 & 0 & 0 & Q_{55} & 0\\ 0 & 0 & 0 & 0 & 0 & Q_{66}\end{bmatrix}^{(k)} \begin{bmatrix}e_1-\alpha_1\Delta T\\ e_2-\alpha_2\Delta T\\ e_3-\alpha_3\Delta T\\ e_4\\ e_5\\ e_6\end{bmatrix}^{(k)} \tag{3}$$

(II) lamina coordinate (x_1, x_2, x_3) constitutive equations

$$\begin{bmatrix}\sigma_{11}\\ \sigma_{22}\\ \sigma_{33}\\ \sigma_{23}\\ \sigma_{31}\\ \sigma_{12}\end{bmatrix}^{(k)} = \begin{bmatrix}C_{11} & C_{12} & C_{13} & 0 & 0 & C_{16}\\ C_{12} & C_{22} & C_{23} & 0 & 0 & C_{26}\\ C_{13} & C_{23} & C_{33} & 0 & 0 & C_{36}\\ 0 & 0 & 0 & C_{44} & C_{45} & 0\\ 0 & 0 & 0 & C_{45} & C_{55} & 0\\ C_{16} & C_{26} & C_{36} & 0 & 0 & C_{66}\end{bmatrix}^{(k)} \begin{bmatrix}e_{11}-\alpha_{11}\Delta T\\ e_{22}-\alpha_{22}\Delta T\\ e_{33}-\alpha_{33}\Delta T\\ 2e_{23}\\ 2e_{31}\\ 2e_{12}-\alpha_{12}\Delta T\end{bmatrix}^{(k)} \tag{4}$$

For convenience, eqn (4) is translated into the following form:

$$\begin{bmatrix}\sigma_{11}\\ \sigma_{22}\\ \sigma_{12}\end{bmatrix}^{(k)} = \begin{bmatrix}\bar{C}_{11} & \bar{C}_{12} & \bar{C}_{16}\\ \bar{C}_{12} & \bar{C}_{22} & \bar{C}_{26}\\ \bar{C}_{16} & \bar{C}_{26} & \bar{C}_{66}\end{bmatrix}^{(k)} \begin{bmatrix}e_{11}-\alpha_{11}\Delta T\\ e_{22}-\alpha_{22}\Delta T\\ 2e_{12}-\alpha_{12}\Delta T\end{bmatrix}^{(k)} + \begin{bmatrix}C_{13}\\ C_{23}\\ C_{36}\end{bmatrix}^{(k)} \left[\frac{\sigma_{33}}{C_{33}}\right]^{(k)} \tag{5a}$$

$$e_{33}^{(k)} = -\left(\frac{C_{13}}{C_{33}}\right)^{(k)}(e_{11}-\alpha_{11}\Delta T)^{(k)} - \left(\frac{C_{23}}{C_{33}}\right)^{(k)}(e_{22}-\alpha_{22}\Delta T)^{(k)}$$

$$-\left(\frac{C_{36}}{C_{33}}\right)^{(k)}(2e_{12}-\alpha_{12}\Delta T)^{(k)} + \left(\frac{\sigma_{33}}{C_{33}}\right)^{(k)} + (\alpha_{33}\Delta T)^{(k)} \tag{5b}$$

$$\begin{bmatrix}2e_{23}\\ 2e_{31}\end{bmatrix}^{(k)} = \begin{bmatrix}\bar{C}_{55} & -\bar{C}_{45}\\ -\bar{C}_{45} & \bar{C}_{44}\end{bmatrix}^{(k)} \begin{bmatrix}\sigma_{23}\\ \sigma_{31}\end{bmatrix}^{(k)}. \tag{5c}$$

(c) Strain–displacement relations

$$e_{ij}^{(k)} = \frac{1}{2}(u_{i,j}^{(k)} + u_{j,i}^{(k)}). \tag{6}$$

(d) Interface continuity conditions

$$u_i^{(k)} = u_i^{(k+1)} \quad \text{and} \quad \sigma_{3i}^{(k)} = \sigma_{3i}^{(k+1)} \quad k = 1, 2, \ldots, N-1. \tag{7}$$

(e) Upper and lower surface stress conditions

$$\sigma_{3i}^{(1)} = P_i^{+} \quad \text{on} \quad x_3 = \frac{h}{2} \tag{8a}$$

$$\sigma_{3i}^{(N)} = P_i^{-} \quad \text{on} \quad x_3 = -\frac{h}{2}. \tag{8b}$$

The basis of a new laminated plate thermoelastic response theory is facilitated by the mixed variational principle (Reissner, 1984) applied to the N-layered composite plate:

$$\iint_D \left[\sum_{k=1}^{N} \int_{A^{(k)}} \{\delta e_{ij}^{(k)} \sigma_{ij}^{(k)} + [u_{3,\alpha}^{(k)} + u_{\alpha,3}^{(k)} - 2e_{3\alpha}^{(k)}(\cdots)]\delta\sigma_{3\alpha}^{(k)} + [u_{3,3}^{(k)} - e_{33}^{(k)}(\cdots)]\delta\sigma_{33}^{(k)}\}\, \mathrm{d}x_3 \right] \mathrm{d}x_1\, \mathrm{d}x_2$$

$$= \iint_D \left[\sum_{k=1}^{N} \int_{A^{(k)}} \delta u_i^{(k)} f_i^{(k)}\, \mathrm{d}x_3 \right] \mathrm{d}x_1\, \mathrm{d}x_2 + \iint_D \left[\delta u_i^{(1)} \left(x_1, x_2, \frac{h}{2} \right) P_i^+ \right.$$

$$\left. - \delta u_i^{(N)} \left(x_1, x_2, -\frac{h}{2} \right) P_i^- \right] \mathrm{d}x_1\, \mathrm{d}x_2 + \int_{\partial D_T} \left[\sum_{k=1}^{N} \int_{A^{(k)}} \delta u_i^{(k)\,\nu} P_i^{(k)}\, \mathrm{d}x_3 \right] \mathrm{d}s \quad (9)$$

where ∂D_T denotes the boundary of domain D with outward normal ν_α on which tractions $^{\nu}P_i$ are prescribed. $\sigma_{3i}^{(k)}$ denote the approximate transverse stresses and $e_{3i}^{(k)}(\cdots)$ are given by eqns (5b, c). Due to the nature of Reissner's mixed variational principle, eqns (5a) are taken to be the definitions of $\sigma_{\alpha\beta}^{(k)}$ used in connection with (9).

Temperature change, displacement and transverse stress fields

Temperature change ΔT is considered to be linear through the thickness of the plate and is given by

$$\Delta T = T_0(x_1, x_2) + x_3 T_1(x_1, x_2). \quad (10)$$

The appropriate functions used in connection with Reissner's mixed variational principle, eqn (9), are chosen to be:

(a) Displacement field

Piecewise linear continuous in-plane displacement distributions are assumed, as shown in Fig. 2:

$$u_\alpha^{(k)}(x_i) = U_\alpha^{(k-1)}(x_\beta) g_1^{(k)}(x_3^{(k)}) + U_\alpha^{(k)}(x_\beta) g_2^{(k)}(x_3^{(k)}) \quad (11a)$$

$$u_3^{(k)}(x_i) = U_3(x_\beta), \quad (11b)$$

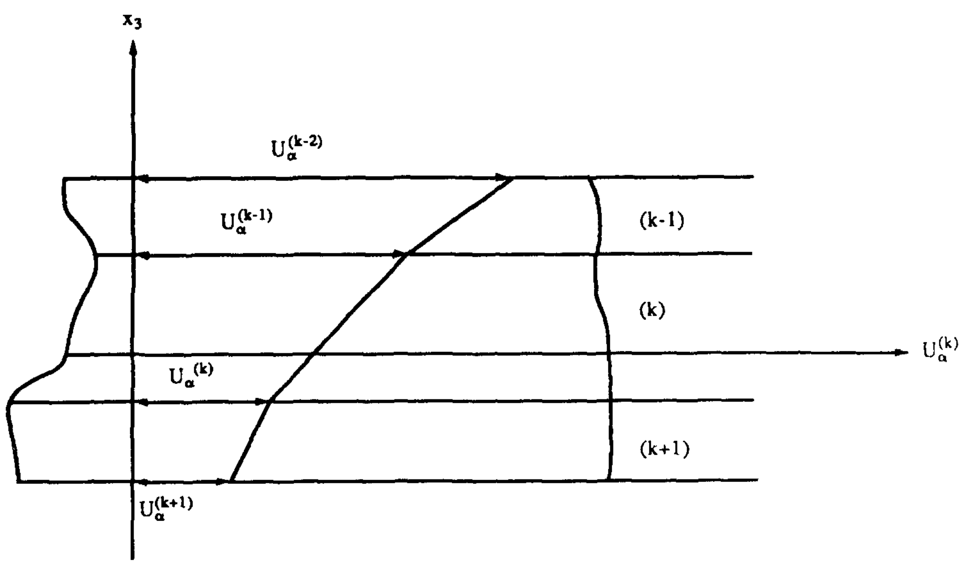

Fig. 2. Approximation of in-plane displacements.

where

$$g_\alpha^{(k)}(x_3^{(k)}) \equiv \frac{1}{2}+(-1)^{\alpha+1}\frac{x_3^{(k)}}{n^{(k)}h} \tag{12}$$

and $x_3^{(k)}$ is a local x_3 coordinate system with its origin at the center $x_{30}^{(k)}$ of the kth layer, i.e.

$$x_3^{(k)} \equiv x_3 - x_{30}^{(k)}. \tag{13}$$

From eqns (11a) and (12), it is seen that $U_\alpha^{(k)}$ ($k = 1, 2, \ldots, N-1$); $U_\alpha^{(0)}$ and $U_\alpha^{(N)}$ represent the values of $u_\alpha^{(k)}$ at the interfaces, and top and bottom surfaces of the plate, respectively. Also, eqns (11) satisfy the interface displacement continuity conditions equation (7a).

(b) Transverse stress field

$$\sigma_{3\alpha}^{(k)}(x_i) = Q_\alpha^{(k)}(x_\beta)F_i(Z)+P_\alpha^{(k-1)}(x_\beta)F_2(Z)+P_\alpha^{(k)}(x_\beta)F_3(Z) \tag{14a}$$

$$\sigma_{33}^{(k)}(x_i) \equiv 0, \tag{14b}$$

where

$$F_i(Z) = \frac{3}{2n^{(k)}h}(1-Z^2) \tag{15a}$$

$$F_i(Z) = \frac{3}{4}Z^2+\frac{1}{2}(-1)^iZ-\frac{1}{4}, \quad i = 2,3 \tag{15b}$$

and

$$Z \equiv \frac{2x_3^{(k)}}{n^{(k)}h}; \quad -1 \leqslant Z \leqslant 1. \tag{16}$$

Also,

$$Q_\alpha^{(k)} \equiv \int_{A^{(k)}} \sigma_{3\alpha}^{(k)}\,\mathrm{d}x_3. \tag{17}$$

In eqn (14a), $P_\alpha^{(k-1)}$ and $P_\alpha^{(k)}$ are the values of $\sigma_{3\alpha}^{(k)}$ at the top and bottom surfaces of the kth layer, respectively.

From eqn (8), one has

$$P_i^{(0)} = P_i^+ \quad \text{and} \quad P_i^{(N)} = P_i^-. \tag{18}$$

Equations (14) satisfy the interface stress continuity conditions, eqn (7b).

Laminated plate equations

Substituting eqns (11) and (14) into eqn (9) and using Gauss's theorem, one obtains:

(a) Equilibrium equations

$$\frac{1}{2}N_{\beta\alpha,\beta}^{(1)}+\frac{1}{n^{(1)}h}(M_{\beta\alpha,\beta}^{(1)}-N_{3\alpha}^{(1)})+\frac{1}{2}F_\alpha^{N(1)}+\frac{1}{n^{(1)}h}F_\alpha^{M(1)}+P_\alpha^+ = 0 \tag{19a}$$

$$\frac{1}{2}(N^{(k)}_{\beta\alpha,\beta}+N^{(k+1)}_{\beta\alpha,\beta})-\frac{1}{h}\left(\frac{M^{(k)}_{\beta\alpha,\beta}}{n^{(k)}}-\frac{M^{(k+1)}_{\beta\alpha,\beta}}{n^{(k+1)}}\right)+\frac{1}{h}\left(\frac{N^{(k)}_{3\alpha}}{n^{(k)}}-\frac{N^{(k+1)}_{3\alpha}}{n^{(k+1)}}\right)+\frac{1}{2}(F^{N(k)}_{\alpha}+F^{N(k+1)}_{\alpha})$$

$$-\frac{1}{h}\left(\frac{F^{M(k)}_{\alpha}}{n^{(k)}}-\frac{F^{M(k+1)}_{\alpha}}{n^{(k+1)}}\right)=0;\quad k=1,2,\ldots,N-1 \quad (19b)$$

$$\frac{1}{2}N^{(N)}_{\beta\alpha,\beta}-\frac{1}{n^{(N)}h}(M^{(N)}_{\beta\alpha,\beta}-N^{(N)}_{3\alpha})+\frac{1}{2}F^{N(N)}_{\alpha}-\frac{1}{n^{(N)}h}F^{M(N)}_{\alpha}-P^{-}_{\alpha}=0 \quad (19c)$$

$$\sum_{k=1}^{N}N^{(k)}_{3\alpha,\alpha}+F^{N}_{3}+P^{+}_{3}-P^{-}_{3}=0, \quad (19d)$$

where

$$(N^{(k)}_{\alpha\beta},M^{(k)}_{\alpha\beta})\equiv\int_{A^{(k)}}(1,x^{(k)}_{3})\sigma^{(k)}_{\alpha\beta}\,\mathrm{d}x_3 \quad (20a)$$

$$N^{(k)}_{3\alpha}\equiv\int_{A^{(k)}}\sigma^{(k)}_{3\alpha}\,\mathrm{d}x_3 \quad (20b)$$

$$(F^{N(k)}_{\alpha},F^{M(k)}_{\alpha})\equiv\int_{A^{(k)}}(1,x^{(k)}_{3})f^{(k)}_{\alpha}\,\mathrm{d}x_3 \quad (20c)$$

$$F^{N}_{3}\equiv\sum_{k=1}^{N}\int_{A_{(k)}}f^{(k)}_{3}\,\mathrm{d}x_3. \quad (20d)$$

(b) Boundary conditions

Specify

$$U^{(k)}_{\alpha}\quad\text{or}\quad\left[\frac{1}{2}(N^{(k)}_{\beta\alpha}+N^{(k+1)}_{\beta\alpha})-\frac{1}{h}\left(\frac{M^{(k)}_{\beta\alpha}}{n^{(k)}}-\frac{M^{(k+1)}_{\beta\alpha}}{n^{(k+1)}}\right)\right]v_{\beta}. \quad (21a)$$

Specify

$$U_3\quad\text{or}\quad\sum_{k=1}^{N}N^{(k)}_{3\alpha}v_{\alpha}. \quad (21b)$$

Equations (21a,b) constitute $(2N+3)$ conditions. It can be seen that the natural edge traction boundary conditions are coupled, i.e. force and moment resultants acting on two adjacent layers are involved.

(c) Constitutive relations

$$Q^{(k)}_{1}-\left(\frac{\bar{C}_{45}}{\bar{C}_{44}}\right)^{(k)}Q^{(k)}_{2}-\frac{n^{(k)}h}{12}(P^{(k-1)}_{1}+P^{(k)}_{1})$$

$$+\frac{n^{(k)}h}{12}\left(\frac{\bar{C}_{45}}{\bar{C}_{44}}\right)^{(k)}(P^{(k-1)}_{2}+P^{(k)}_{2})=\frac{5}{6\bar{C}^{(k)}_{44}}(U^{(k-1)}_{1}-U^{(k)}_{1}+n^{(k)}hU_{3,1}) \quad (22a)$$

$$-\left(\frac{\bar{C}_{45}}{\bar{C}_{55}}\right)^{(k)}Q^{(k)}_{1}+Q^{(k)}_{2}+\frac{n^{(k)}h}{12}\left(\frac{\bar{C}_{45}}{\bar{C}_{55}}\right)^{(k)}(P^{(k-1)}_{1}+P^{(k)}_{1})$$

$$-\frac{n^{(k)}h}{12}(P^{(k-1)}_{2}+P^{(k)}_{2})=\frac{5}{6\bar{C}^{(k)}_{55}}(U^{(k-1)}_{2}-U^{(k)}_{2}+n^{(k)}hU_{3,2}) \quad (22b)$$

$$\frac{1}{10}(\bar{C}_{44}^{(k)}Q_1^{(k)}+\bar{C}_{44}^{(k+1)}Q_1^{(k+1)})-\frac{1}{10}(\bar{C}_{45}^{(k)}Q_2^{(k)}+\bar{C}_{45}^{(k+1)}Q_2^{(k+1)})$$

$$+\frac{h}{30}[n^{(k)}\bar{C}_{44}^{(k)}P_1^{(k-1)}-4(n^{(k)}\bar{C}_{44}^{(k)}+n^{(k+1)}\bar{C}_{44}^{(k+1)})P_1^{(k)}+n^{(k+1)}\bar{C}_{44}^{(k+1)}P_1^{(k+1)}]$$

$$-\frac{h}{30}[n^{(k)}\bar{C}_{45}^{(k)}P_2^{(k-1)}-4(n^{(k)}\bar{C}_{45}^{(k)}+n^{(k+1)}\bar{C}_{45}^{(k+1)})P_2^{(k)}+n^{(k+1)}\bar{C}_{45}^{(k+1)}P_2^{(k+1)}]=0 \quad (22c)$$

$$-\frac{1}{10}(\bar{C}_{45}^{(k)}Q_1^{(k)}+\bar{C}_{45}^{(k+1)}Q_1^{(k+1)})+\frac{1}{10}(\bar{C}_{55}^{(k)}Q_2^{(k)}+\bar{C}_{55}^{(k+1)}Q_2^{(k+1)})$$

$$-\frac{h}{30}[n^{(k)}\bar{C}_{45}^{(k)}P_1^{(k-1)}-4(n^{(k)}\bar{C}_{45}^{(k)}+n^{(k+1)}\bar{C}_{45}^{(k+1)})P_1^{(k)}+n^{(k+1)}\bar{C}_{45}^{(k+1)}P_1^{(k+1)}]$$

$$+\frac{h}{30}[n^{(k)}\bar{C}_{55}^{(k)}P_2^{(k-1)}-4(n^{(k)}\bar{C}_{55}^{(k)}+n^{(k+1)}\bar{C}_{55}^{(k+1)})P_2^{(k)}+n^{(k+1)}\bar{C}_{55}^{(k+1)}P_2^{(k+1)}]=0. \quad (22d)$$

In eqns (22a, b), k ranges from 1 to N, while in eqns (22c, d), k ranges from 1 to $(N-1)$. Equations (22) can be solved for $Q_\alpha^{(k)}$ and $P_\alpha^{(k)}$ in terms of $U_\alpha^{(k)}$ and $U_{3,\alpha}$. As a result, the quantities $N_{3\alpha}^{(k)}$ can be determined as functions of these displacement variables. Such expressions will automatically include appropriate shear correction factors by virtue of Reissner's mixed variational principle.

The remaining constitutive equations for $N_{\alpha\beta}^{(k)}$ and $M_{\alpha\beta}^{(k)}$ are obtained by substituting eqns (5a), (6) and (11) into (20a) to yield

$$\begin{bmatrix} N_{11} \\ N_{22} \\ N_{12} \end{bmatrix}^{(k)} = \frac{n^{(k)}h}{2}\begin{bmatrix} \bar{C}_{11} & \bar{C}_{12} & \bar{C}_{16} \\ \bar{C}_{12} & \bar{C}_{22} & \bar{C}_{26} \\ \bar{C}_{16} & \bar{C}_{26} & \bar{C}_{66} \end{bmatrix}^{(k)} \begin{bmatrix} U_{1,1}^{(k-1)}+U_{1,1}^{(k)}-2\alpha_{11}^{(k)}(T_0+x_{30}^{(k)}T_1) \\ U_{2,2}^{(k-1)}+U_{2,2}^{(k)}-2\alpha_{22}^{(k)}(T_0+x_{30}^{(k)}T_1) \\ U_{1,2}^{(k-1)}+U_{2,1}^{(k-1)}+U_{1,2}^{(k)}+U_{2,1}^{(k)}-2\alpha_{12}^{(k)}(T_0+x_{30}^{(k)}T_1) \end{bmatrix} \quad (23a)$$

$$\begin{bmatrix} M_{11} \\ M_{22} \\ M_{12} \end{bmatrix}^{(k)} = \frac{(n^{(k)}h)^2}{12}\begin{bmatrix} \bar{C}_{11} & \bar{C}_{12} & \bar{C}_{16} \\ \bar{C}_{12} & \bar{C}_{22} & \bar{C}_{26} \\ \bar{C}_{16} & \bar{C}_{26} & \bar{C}_{66} \end{bmatrix}^{(k)} \begin{bmatrix} U_{1,1}^{(k-1)}-U_{1,1}^{(k)}-\alpha_{11}^{(k)}n^{(k)}hT_1 \\ U_{2,2}^{(k-1)}-U_{2,2}^{(k)}-\alpha_{22}^{(k)}n^{(k)}hT_1 \\ U_{1,2}^{(k-1)}+U_{2,1}^{(k-1)}-U_{1,2}^{(k)}-U_{2,1}^{(k)}-\alpha_{12}^{(k)}n^{(k)}hT_1 \end{bmatrix}. \quad (23b)$$

3. BENDING OF CROSS-PLY RECTANGULAR PLATES

In this section, the present theory is applied to the bending problem of cross-ply rectangular plates. The plate is simply supported at the ends $x_1 = 0$ and $L1$, $x_2 = 0$ and $L2$. The prescribed boundary conditions on the top and bottom surfaces of the plate are

$$P_1^+ = P_2^+ = P_3^+ = 0, \quad \text{on} \quad x_3 = \frac{h}{2} \quad (24a)$$

$$P_1^- = P_2^- = P_3^- = 0, \quad \text{on} \quad x_3 = -\frac{h}{2}. \quad (24b)$$

A sinusoidal distribution of the thermal loadings is considered, which for the present case takes the form

$$(T_0, T_1) = (\bar{T}_0, \bar{T}_1)\sin\frac{\pi x_1}{L1}\sin\frac{\pi x_2}{L2}. \quad (25)$$

The boundary conditions for the simply supported ends are, from eqns (21), at $x_1 = 0, L1$

$$U_3 = 0 \quad \text{and} \quad \frac{1}{2}(N_{11}^{(k)}+N_{11}^{(k+1)})-\frac{1}{h}\left(\frac{M_{11}^{(k)}}{n^{(k)}}-\frac{M_{11}^{(k+1)}}{n^{(k+1)}}\right)=0 \tag{26a}$$

at $x_2 = 0, L2$

$$U_3 = 0 \quad \text{and} \quad \frac{1}{2}(N_{22}^{(k)}+N_{22}^{(k+1)})-\frac{1}{h}\left(\frac{M_{22}^{(k)}}{n^{(k)}}-\frac{M_{22}^{(k+1)}}{n^{(k+1)}}\right)=0. \tag{26b}$$

For the cross-ply plates, there holds

$$\bar{C}_{16}^{(k)}=\bar{C}_{26}^{(k)}=C_{36}^{(k)}=0 \quad \bar{C}_{45}^{(k)}=0 \quad \bar{C}_{66}^{(k)}=C_{66}^{(k)} \quad \bar{C}_{44}^{(k)}=\frac{1}{C_{55}^{(k)}} \quad \bar{C}_{55}^{(k)}=\frac{1}{C_{44}^{(k)}} \quad \alpha_{12}^{(k)}=0. \tag{27}$$

Equations (22a, c) and (22b, d) can be written in matrix form as

$$\{Q_1\}-h[B_1]\{P_1\}=b \tag{28a}$$

$$[D_1]\{Q_1\}+h[F_1]\{P_1\}=0 \tag{28b}$$

$$\{Q_2\}-h[BB_1]\{P_2\}=bb \tag{28c}$$

$$[DD_1]\{Q_2\}+h[FF_1]\{P_2\}=0, \tag{28d}$$

where

$$\{Q_1\}\equiv[Q_1^{(1)},Q_1^{(2)},\ldots,Q_1^{(N)}]^T \quad \{P_1\}\equiv[P_1^{(1)},P_1^{(2)},\ldots,P_1^{(N-1)}]^T \tag{29a}$$

$$\{Q_2\}\equiv[Q_2^{(1)},Q_2^{(2)},\ldots,Q_2^{(N)}]^T \quad \{P_2\}\equiv[P_2^{(1)},P_2^{(2)},\ldots,P_2^{(N-1)}]^T \tag{29b}$$

and $[B_1]([BB_1])$, $[D_1]([DD_1])$ and $[F_1]([FF_1])$ are matrices of dimensions $N\times(N-1)$, $(N-1)\times N$ and $(N-1)\times(N-1)$, respectively. The matrices $[B_1]$, $[D_1]$, $[F_1]$ and $[BB_1]$, $[DD_1]$, $[FF_1]$ are only functions of $n^{(k)}$, $C_{55}^{(k)}$ and $n^{(k)}$, $C_{44}^{(k)}$, respectively.

The right-hand side of eqns (28a) and (28c) contain the displacement variables $U_1^{(k)}$, $U_{3,1}$ and $U_2^{(k)}$, $U_{3,2}$, respectively.

Equations (28) can be solved for $Q_1^{(k)}$, $P_1^{(k)}$ and $Q_2^{(k)}$, $P_2^{(k)}$ to yield

$$h\{P_1\}=-[F_1]^{-1}[D_1]\{Q_1\} \tag{30a}$$

$$\{Q_1\}=([I]+[B_1][F_1]^{-1}[D_1])^{-1}b \tag{30b}$$

$$h\{P_2\}=-[FF_1]^{-1}[DD_1]\{Q_2\} \tag{30c}$$

$$\{Q_2\}=([I]+[BB_1][FF_1]^{-1}[DD_1])^{-1}bb, \tag{30d}$$

where $[I]$ is the $N\times N$ identity matrix.

Using surface boundary conditions (24), the equilibrium equations (19) for bending of rectangular plates in the absence of body forces reduce to

$$\frac{1}{2}(N_{11,1}^{(1)}+N_{21,2}^{(1)})+\frac{1}{n^{(1)}h}[(M_{11,1}^{(1)}+M_{21,2}^{(1)})-N_{31}^{(1)}]=0 \tag{31a}$$

$$\frac{1}{2}(N_{12,1}^{(1)}+N_{22,2}^{(1)})+\frac{1}{n^{(1)}h}[(M_{12,1}^{(1)}+M_{22,2}^{(1)})-N_{32}^{(1)}]=0 \tag{31b}$$

$$\frac{1}{2}[(N_{11,1}^{(k)}+N_{11,1}^{(k+1)})+(N_{21,2}^{(k)}+N_{21,2}^{(k+1)})]-\frac{1}{h}\left[\left(\frac{M_{11,1}^{(k)}}{n^{(k)}}-\frac{M_{11,1}^{(k+1)}}{n^{(k+1)}}\right)\right.$$

$$\left.+\left(\frac{M_{21,2}^{(k)}}{n^{(k)}}-\frac{M_{21,2}^{(k+1)}}{n^{(k+1)}}\right)\right]+\frac{1}{h}\left(\frac{N_{31}^{(k)}}{n^{(k)}}-\frac{N_{31}^{(k+1)}}{n^{(k+1)}}\right)=0 \quad k=1,2,\ldots,N-1 \tag{31c}$$

$$\frac{1}{2}[(N_{12,1}^{(k)}+N_{12,1}^{(k+1)})+(N_{22,2}^{(k)}+N_{22,2}^{(k+1)})]-\frac{1}{h}\left[\left(\frac{M_{12,1}^{(k)}}{n^{(k)}}-\frac{M_{12,1}^{(k+1)}}{n^{(k+1)}}\right)\right.$$

$$\left.+\left(\frac{M_{22,2}^{(k)}}{n^{(k)}}-\frac{M_{22,2}^{(k+1)}}{n^{(k+1)}}\right)\right]+\frac{1}{h}\left(\frac{N_{32}^{(k)}}{n^{(k)}}-\frac{N_{32}^{(k+1)}}{n^{(k+1)}}\right)=0 \quad k=1,2,\ldots,N-1 \tag{31d}$$

$$\frac{1}{2}(N_{11,1}^{(N)}+N_{21,2}^{(N)})-\frac{1}{n^{(N)}h}[(M_{11,1}^{(N)}+M_{21,2}^{(N)})-N_{31}^{(N)}]=0 \tag{31e}$$

$$\frac{1}{2}(N_{12,1}^{(N)}+N_{22,2}^{(N)})-\frac{1}{n^{(N)}h}[(M_{12,1}^{(N)}+M_{22,2}^{(N)})-N_{32}^{(N)}]=0 \tag{31f}$$

$$\sum_{k=1}^{N}(N_{31,1}^{(k)}+N_{32,2}^{(k)})=0. \tag{31g}$$

Boundary conditions (26) and the nature of thermal loading suggest the following expressions for the displacements:

$$U_1^{(k)}=h\bar{U}_1^{(k)}\cos\frac{\pi x_1}{L1}\sin\frac{\pi x_2}{L2} \tag{32a}$$

$$U_2^{(k)}=h\bar{U}_2^{(k)}\sin\frac{\pi x_1}{L1}\cos\frac{\pi x_2}{L2} \tag{32b}$$

$$U_3=h\bar{U}_3\sin\frac{\pi x_1}{L1}\sin\frac{\pi x_2}{L2}, \tag{32c}$$

where $\bar{U}_1^{(k)}$, $U_2^{(k)}$ and $\bar{U}_3$ are nondimensional quantities by definition. It is easily proven that the boundary conditions (26) are satisfied when eqns (32) are substituted therein.

Finally, inserting (32) into the constitutive equations (30b, d) and (23a, b), in which $\bar{C}_{16}^{(k)}=\bar{C}_{26}^{(k)}=0$, $\bar{C}_{66}^{(k)}=C_{66}^{(k)}$, and these in turn into the equilibrium equations (31), yields a system of $(2N+3)$ algebraic equations with the $(2N+3)$ nondimensional amplitudes $\bar{U}_1^{(k)}$, $\bar{U}_2^{(k)}$ and $\bar{U}_3$ as unknowns. This system is conveniently written in matrix form as

$$[X]\bar{U}=F, \tag{33}$$

where

$$\bar{U}=[\bar{U}_1^{(0)},\bar{U}_1^{(1)},\ldots,\bar{U}_1^{(N)},\bar{U}_2^{(0)},\bar{U}_2^{(1)},\ldots,\bar{U}_2^{(N)},\bar{U}_3]^T$$

and $[X]$ is a $(2N+3)\times(2N+3)$ matrix.

4. NUMERICAL RESULTS AND DISCUSSION

Numerical results for various different cross-ply lamination schemes are presented. It was assumed that the thickness and the material for all the laminae are the same, having the following characteristics:

$$E_1=25E_2 \quad E_3=E_2 \quad G_{12}=G_{13}=0.5E_2$$

$$G_{23}=0.2E_2 \quad \nu_{12}=\nu_{13}=\nu_{23}=0.25 \quad \alpha_2/\alpha_1=3;$$

T_0 is considered as 0 throughout the calculations.

The following nondimensional deflection and stresses have been used:

$$\bar{u}_3 = u_3\left(\frac{L1}{2}, \frac{L2}{2}\right) \times 10/(\alpha_1 \bar{T}_1 L1^2)$$

$$\bar{\sigma}_{11}^{(k)} = \sigma_{11}^{(k)}\left(\frac{L1}{2}, \frac{L2}{2}, x_3\right) \times 10/(\alpha_1 \bar{T}_1 E_2 L1)$$

$$\bar{\sigma}_{22}^{(k)} = \sigma_{22}^{(k)}\left(\frac{L1}{2}, \frac{L2}{2}, x_3\right) \times 10/(\alpha_1 \bar{T}_1 E_2 L1)$$

$$\bar{\sigma}_{12}^{(k)} = \sigma_{12}^{(k)}(0, 0, x_3) \times 10/(\alpha_1 \bar{T}_1 E_2 L1)$$

$$\bar{\sigma}_{31}^{(k)} = \sigma_{31}^{(k)}\left(0, \frac{L2}{2}, x_3\right) \times 10/(\alpha_1 \bar{T}_1 E_2 L1)$$

$$\bar{\sigma}_{23}^{(k)} = \sigma_{23}^{(k)}\left(\frac{L1}{2}, 0, x_3\right) \times 10/(\alpha_1 \bar{T}_1 E_2 L1). \tag{34}$$

Also

$$\bar{x}_3 = \frac{x_3}{h} \quad \text{and} \quad S_1 = \frac{L1}{h}. \tag{35}$$

Some numerical results are compared with those obtained using the high-order theory by Khdeir and Reddy (1991) and the first-order zig-zag theory by Liu *et al.* (1994), which is developed by superposing to the linear variations of the Reissner–Mindlin theory a zig-zag in-plane displacement variation across the plate thickness.

In the first-order zig-zag theory, the displacements are expressed by

$$u_\alpha^{(k)}(x_i) = U_\alpha(x_\beta) + \Psi_\alpha(x_\beta)x_3 + S_\alpha(x_\beta)(-1)^k \frac{2x_3^{(k)}}{n^{(k)}h} \tag{36a}$$

$$u_3^{(k)}(x_i) = U_3(x_\beta). \tag{36b}$$

In the various compared curves, the solid line represents the results of the present theory, while the results of the first-order zig-zag theory are shown by a dashed line.

For a symmetric three-layer square (0/90/0, $L1 = L2$) and five-layer rectangular (0/90/0/90/0, $L2/L1 = 3$) and antisymmetric four-layer square (0/90/0/90, $L1 = L2$) and 10-layer square ($0/90, \ldots, _{10\ \text{layers}}$, $L1 = L2$) cross-ply laminates, Table 1 shows the values of the central deflection obtained from the different theories for the side-to-thickness ratio $S_1 = 5, 10$.

Table 1. Central deflection $\bar{u}_3$ for symmetric three- and five-layer and antisymmetric four- and 10-layer cross-ply laminates ($S_1 = 5, 10$)

	$N = 3$		$N = 5$		$N = 4$		$N = 10$	
Theories	$S_1 = 5$	$S_1 = 10$	$S_1 = 5$	$S_1 = 10$	$S_1 = 5$	$S_1 = 10$	$S_1 = 5$	$S_1 = 10$
Present theory	1.0917	1.0524	1.05536	1.1085	1.07186	1.04881	1.3767	1.03429
First-order zig-zag theory	1.0917	1.0524	1.1554	1.1102	1.04249	1.04500	1.03226	1.03302
High-order theory	1.0874	1.0499	—	—	—	—	1.0336	1.0333

Figures 3–5 give the curves of $\bar{u}_3$ versus width to thickness ratio S_1 for the symmetric three- and five-layer and antisymmetric four-layer plates, respectively. As observed, the present theory and the first-order zig-zag theory yield exactly the same numerical results for the three-layer plate; for the other plates, very close agreement is found between both theories with the increase of side-to-thickness ratio.

Figures 6–10 show the in-plane and transverse shear stress distributions across the thickness for the symmetric three-layer laminate for $S_1 = 10$; both the theories also yield exactly the same results.

The thickness variations of the in-plane stresses for the symmetric five-layer laminate for $S_1 = 10$ are shown in Figs 11–13, where very close agreement between both theories is obtained.

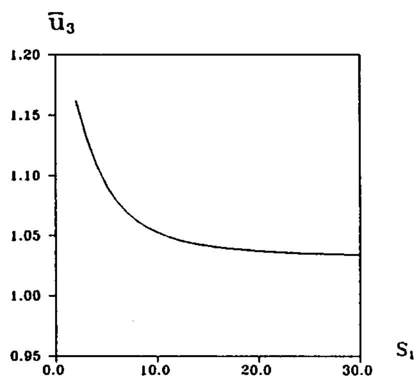

Fig. 3. Center deflection vs side-to-thickness of a (0/90/0) square plate.

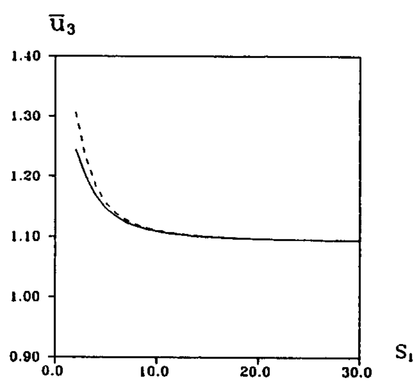

Fig. 4. Center deflection vs side-to-thickness of a (0/90/0/90/0) rectangular plate ($L2/L1 = 3$).

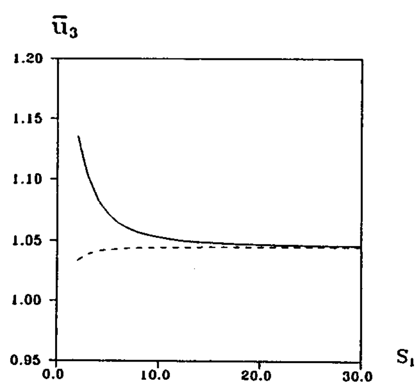

Fig. 5. Center deflection vs side-to-thickness of a (0/90/0/90) square plate.

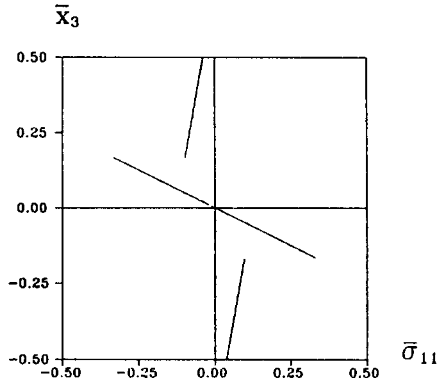

Fig. 6. Thickness variation of in-plane stress $\bar{\sigma}_{11}$ of a symmetric three-layer cross-ply square plate for $L1/h = 10$.

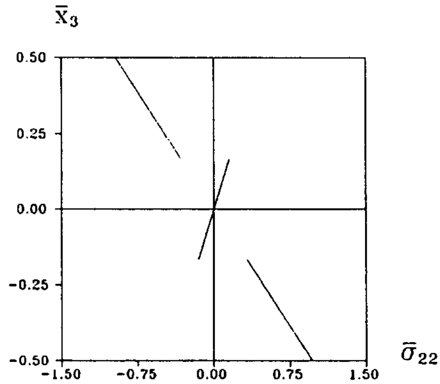

Fig. 7. Thickness variation of in-plane stress $\bar{\sigma}_{22}$ of a symmetric three-layer cross-ply square plate for $L1/h = 10$.

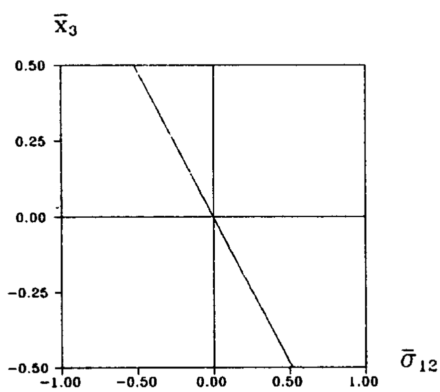

Fig. 8. Thickness variation of in-plane stress $\bar{\sigma}_{12}$ of a symmetric three-layer cross-ply square plate for $L1/h = 10$.

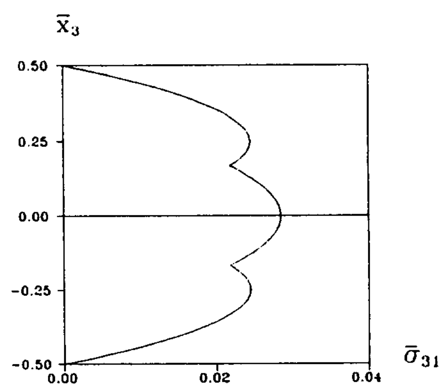

Fig. 9. Thickness variation of transverse shear stress $\bar{\sigma}_{31}$ of a symmetric three-layer cross-ply square plate for $L1/h = 10$.

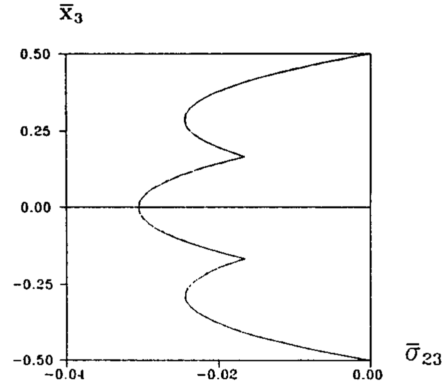

Fig. 10. Thickness variation of transverse shear stress $\bar{\sigma}_{23}$ of a symmetric three-layer cross-ply square plate for $L1/h = 10$.

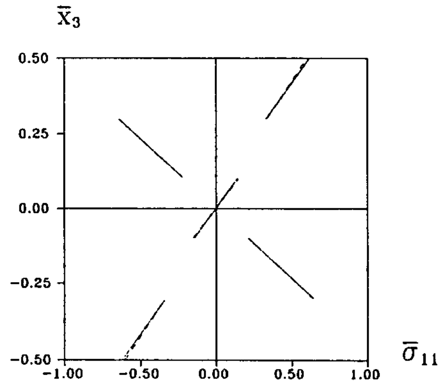

Fig. 11. Thickness variation of in-plane stress $\bar{\sigma}_{11}$ of a symmetric five-layer cross-ply square plate for $L1/h = 10$, $L2/L1 = 3$.

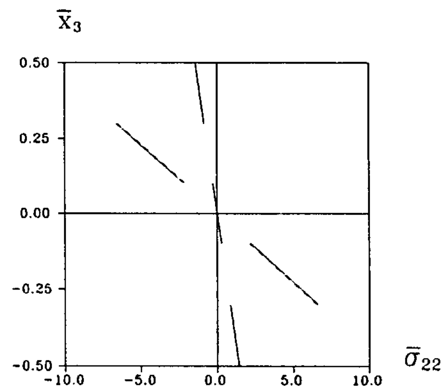

Fig. 12. Thickness variation of in-plane stress $\bar{\sigma}_{22}$ of a symmetric five-layer cross-ply square plate for $L1/h = 10$, $L2/L1 = 3$.

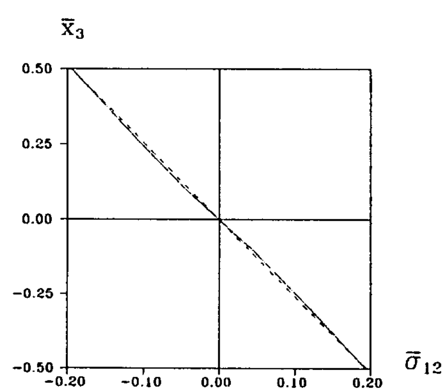

Fig. 13. Thickness variation of in-plane stress $\bar{\sigma}_{12}$ of a symmetric five-layer cross-ply square plate for $L1/h = 10$, $L2/L1 = 3$.

Figures 14–16 show the thickness variations of in-plane stresses for an antisymmetric four-layer laminate for $S_1 = 10$, where exact agreement is found between the theories for $\bar{\sigma}_{12}$. However, it is seen that the first-order zig-zag theory deviates significantly from the present theory at the 0° layers for $\bar{\sigma}_{11}$ and at the 90° layers for $\bar{\sigma}_{22}$.

From these results, it is seen that for those symmetric laminate configurations, very good agreement occurs between the present theory and the first-order zig-zag theory, but for those antisymmetric laminate configurations, a discrepancy occurs between both theories. As a possible explanation, the following argument is proposed by Toledano and Murakami (1987). The inclusion of the zig-zag shaped C^0 function was motivated by the displacement microstructure of periodic laminated composites. Obviously, for arbitrary

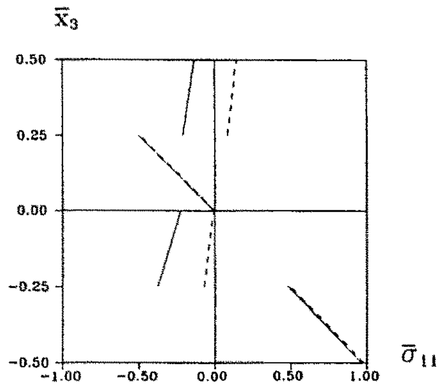

Fig. 14. Thickness variation of in-plane stress $\bar{\sigma}_{11}$ of an antisymmetric four-layer cross-ply square plate for $L1/h = 10$.

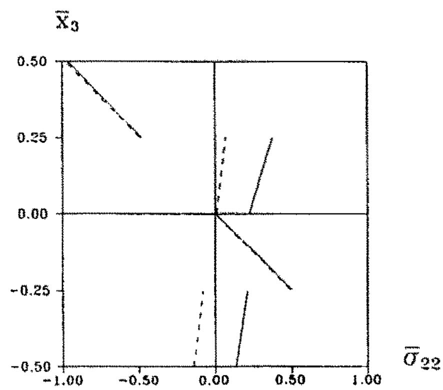

Fig. 15. Thickness variation of in-plane stress $\bar{\sigma}_{22}$ of an antisymmetric four-layer cross-ply square plate for $L1/h = 10$.

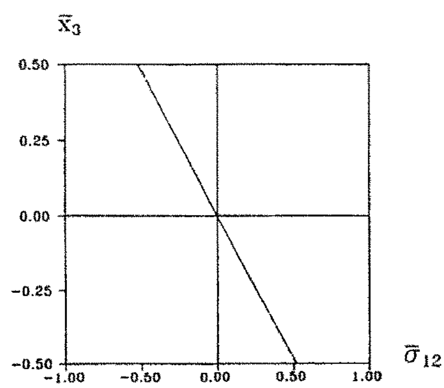

Fig. 16. Thickness variation of in-plane stress $\bar{\sigma}_{12}$ of an antisymmetric four-layer cross-ply square plate for $L1/h = 10$.

laminate configurations, this periodicity is destroyed. Therefore, the first-order zig-zag theory would be expected to break down in these particular cases. This explanation shows that the present theory is improved upon the first-order zig-zag theory.

Some important points are now discussed. The accuracy of the present theory can be improved by dividing each ply into a finite number of sub-layers, but at the expense of increasing computer storage. Also, the proposed theory possesses two main drawbacks, which are, first, the number of equilibrium equations and edge boundary conditions increases with the number of layers, which makes the calculation difficult for those laminates with a large number of layers; second, due to the coupling of the natural edge boundary conditions [see eqn (21)], no clear physical meaning seems to be associated with them.

Finally, it is expected that the thermoelastic problem for arbitrary shaped plates with arbitrary boundary conditions and mechanical and thermal loading cases can be solved using the present theory.

5. CONCLUSION

A composite plate thermoelastic theory was developed by assuming a linear variation of in-plane displacements and a quadratic variation of transverse stresses across each individual lamina. Transverse displacements were kept constant throughout the entire plate thickness. Governing equations and appropriate boundary conditions were then deduced from Reissner's (1984) mixed variational principle. Linear temperature change was assumed through the thickness. The bending problem of cross-ply rectangular plates was analysed using this theory. Values for the central deflection and stresses for symmetric and antisymmetric laminates were presented. Finally, some important points about the present theory were discussed. Despite certain shortcomings, the present theory may prove useful in the investigation of the thermoelastic problem of laminated plates.

REFERENCES

Khdeir, A. A. and Reddy, J. N. (1991). Thermal stresses and deflections of cross-ply laminated plates using refined plate theories. *J. Therm. Stresses* **14**, 4138.

Liu Ping, Zhang Yongwei and Zhang Xiangzhou (1994). Thermoelastic theory for laminated composite plates. *J. Therm. Stresses* (in press).

Pell, W. H. (1946). Thermal deflections of anisotropic thin plates. *Q. Appl. Math.* **4,** 27–44.

Reddy, J. N. and Hsu, Y. S. (1980). Effects of shear deformation and anisotropy on the thermal bending of layered composite plates. *J. Therm. Stresses* **3,** 475–493.

Reissner, E. (1984). On a certain mixed variational principle and a proposed application. *Int. J. Numer. Engng* **20,** 1366–1368.

Stavsky, Y. (1963). Thermoelasticity of heterogeneous aeolotropic plates. *J. Engng Mech. Div. Proc. ASCE* **EM-2,** 89–105.

Stavsky, Y. (1975). Thermoelastic stability of laminated orthotropic circular plates. *Acta Mech.* **22,** 31–51.

Toledano, A and Murakami, H. (1987). A composite plate theory for arbitrary laminate configurations. *J. Appl. Mech.* **54,** 181–189.

Whitney, J. M. and Ashton J. E. (1971). Effect of environment on the elastic response of layered composite plates. *AIAA J.* **9,** 1708–1713.

Wu, C. H. (1978). Thermal deformations and stresses in laminated plates. Master's thesis, University of Kentucky, Lexington.

Wu, C. H. and Tauchert, T. R. (1980a). Thermoelastic analysis of laminated plates. 1: symmetric specially orthotropic laminates. *J. Therm. Stresses* **3,** 247–259.

Wu, C. H. and Tauchert, T. R. (1980b). Thermoelastic analysis of laminated plates. 2: antisymmetric cross-ply and angle-ply laminates. *J. Therm. Stresses* **3,** 365–378.